2016

Heat Transfer and Pressure Drop during Evaporation of R134a in Microchannel Tubes

Houpei Li
ACRC, the University of Illinois, hli84@illinois.edu

Pega Hrnjak
pega@illinois.edu

Heat Transfer and Pressure Drop during Evaporation of R134a in Microchannel Tubes

Houpei LI[1], Pega HRNJAK[12*]

[1] ACRC, University of Illinois,
Urbana, Illinois, USA
hli84@illinois.edu

[2]Creative Thermal Solutions, Inc.,
Urbana, Illinois, USA
pega@illinois.edu

* Corresponding Author

ABSTRACT

The paper presents result for heat transfer and pressure drop in evaporation of R134a in microchannel tubes conducted in a facility with a 6 m long tube, modified to provide realistic situations for refrigerant blends with even the highest glide. The concept of the experimental facility is to measure heat transfer coefficient and pressure drop on the refrigerant side in condensation and evaporation with or without oil. The auto-controlled test line has 6 test sections for testing and 5 conditioning sections to preset the inlet quality of each test section. This facility provides data in the complete process of evaporation (quality from 0 to 1) or condensation (quality from 1 to 0) in a single pass. The secondary fluid in coolant loop for heating or cooling is water. By controlling the inlet water temperature of each test section, both constant wall temperature and constant heat flux conditions or anything in-between can be achieved. The tertiary loop is a chiller loop running with glycol/water mixtures to cool the water and refrigerant.

First results with R134a in this facility show heat transfer coefficient and pressure drop changes with vapor quality and represent excellent starting point (baseline) for explorations of mixtures of low pressure and low GWP refrigerants that are replacements for R410A.

1. INTRODUCTION

Microchannel with smaller hydraulic diameter can increase in-tube heat transfer coefficient and pressure drop. By installing microchannel tubes instead of conventional tubes, the size and weight of heat exchanger can be decreased. In additional, a microchannel has larger surface-area-to-volume-ratio so that it has a higher boiling effect. As the diameter decreased from 10 to 1 millimeter, which are typical conventional tube diameter and microchannel tube diameter respectively, the ratio increased to 10 times. A larger surface-area-to-volume-ratio gives higher on-site boiling effect. Also, the smaller hydraulic diameter in microchannel tubes helps the fluid to wet the whole tube surface. In a conventional tube, the liquid may only fill half of the tube (stratified flow) because of the gravitational force. However, in a tube with the hydraulic diameter smaller than the capillary length scale, the surface tension force can overcome the gravitational force (Triplett et al., 1999). In microchannel tubes, an annular flow or slug flow is more likely to be observed than stratified flow.

2. EXPERIMENTAL FACILITY AND DATA REDUCTION

A new experimental facility has been designed and built to study heat transfer and hydraulic behavior of refrigerants in microchannel tubes. The facility can measure heat transfer coefficient for a given heat flux, mass flux, and wall temperature. In the meantime, data of diabatic pressure drop can be collected. Adiabatic pressure drop can be measured separately, w/o heat load. There are three loops in this facility as shown in Figure 1: refrigerant loop (green loop), coolant (water) loop (blue loop), and chiller (glycol) loop (purple loop).

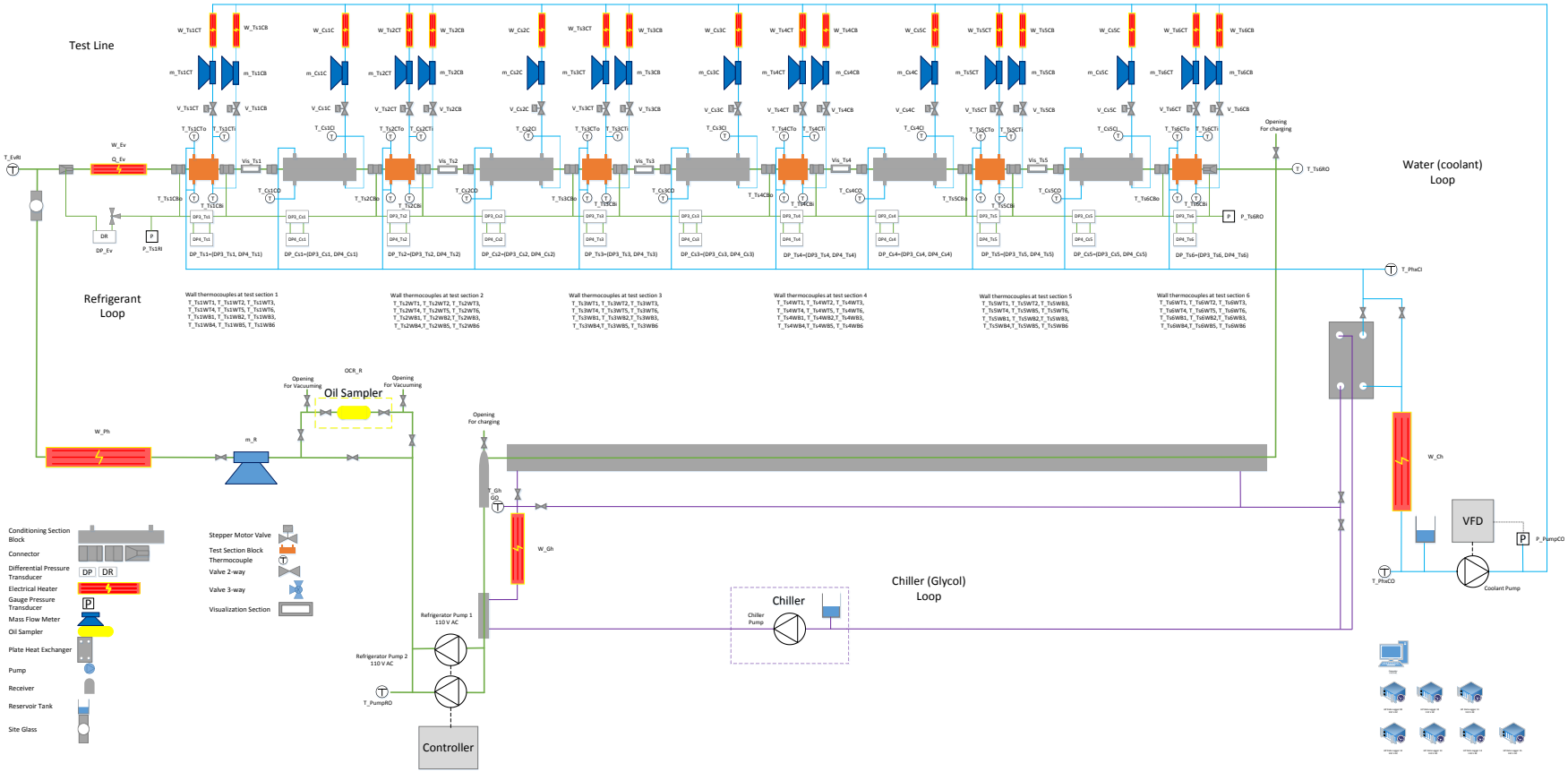

Figure 1 Schematic of the experimental facility

2.1 Refrigerant Loop

Figure 1 shows that subcooled refrigerant is pumped by a two gear pump setup to provide sufficient flow rate and the head to overcome high pressure drop in the microchannel test line. An inline OCR measurement sampler with bypass is installed after the pumps. A Micro Motion CMF010 mass flow meter with the RFT9739 transmitter is used to measure refrigerant flow rate and density. A pre-heater of 2 kW is used to adjust the sub-cooled inlet condition to the test line. The test line consists of one evaporator, six test sections to measure heat transfer coefficient and pressure drop, and five conditioning sections between each test section.

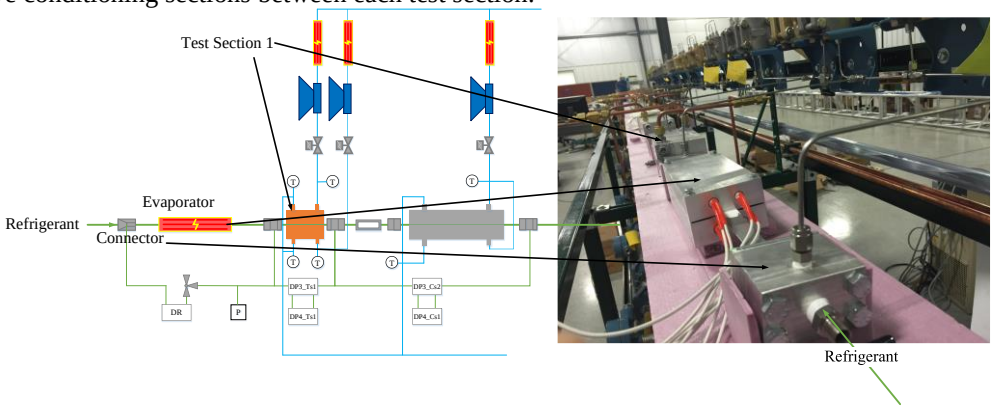

Figure 2 Schematics drawing and view to the entire test line from the inlet with DP transducers on the right

The evaporator and conditioning sections are used for adjusting inlet condition of the following test section as showed more detailed in Figure 2. Starting point is enthalpy of the subcooled liquid in front the evaporator using measured pressure (pressure transducer) and temperature (T-type thermocouple). Heat transferred in the evaporator is determined by the DC system power supply that in addition to supplying power provides measurements of current and voltage and thus power. Quality at the inlet to the first test section is determined based on measured power of the evaporator and refrigerant flow rate. Pressure measured at the inlet to the first test section is a starting point for the pressure of entire test line. Pressure drop through the test section is measured by two differential pressure transducers that are connected to the test line at the connectors. A test section has two heat transfer block. The block is 152.4mm long and with water jacket inside for coolant loop. Two blocks sandwich a microchannel tube and the wall thermocouple is measured by six inserted thermocouple probe in well near the tube on each block. Two blocks are tightened by four long screw bolts with nuts with the same torque (7.6 N-m). Between the blocks and microchannel, the surface cavities are filled with thermal paste CHEMPLEX 1381 DE with reported thermal conductivity with 0.75 $W\text{-}m^{-1}K^{-1}$.

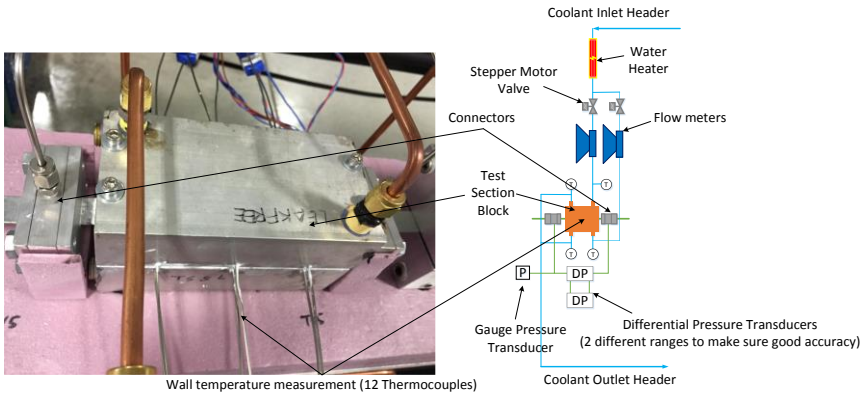

Figure 3 The test section: photo shows actual appearance with six TCs for measurements of wall temperature at each block while schematic drawing shows separate adjustments by stepper motor valves and measurements of coolant flow through top and bottom blocks

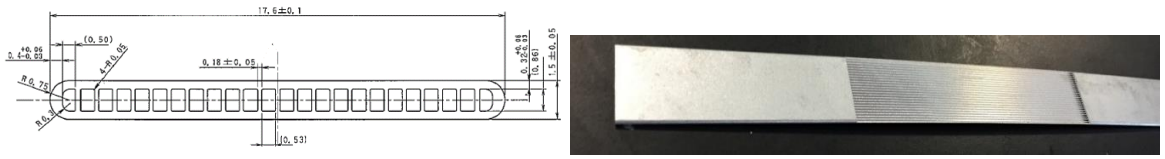

Figure 4 Mechanical drawing and photo of the microchannel tube on the facility

In each test section, the microchannel tube is 181.8 mm long combined with heated length (152.4 mm) and the rest in connectors. The tube has 22 0.83-by-0.56 mm rectangular ports and 2 smaller ports as shown in figure 4. After the test section, refrigerant goes through visualization section and conditioning section. The conditioning section has the same design of test section but longer in length (400 mm), without wall temperature TC well, and is not tightened.

The heat transfer rate of the conditioning section is determined by the flow rate of coolant into the heat transfer block and the temperature difference of coolant at the outlet and inlet of the block. That heat transfer rate combined with refrigerant mass flow rate and pressure determines increase in quality within the conditioning section. As said above, pressure is determined by adding (or subtracting) pressure drop in each section. When all pressure drops are added together they should be a difference between the readings of pressure transducers at the inlet and outlet of the test line.

An opening located at the outlet of the test line is for charging and evacuation. A co-axial condenser (round tube to microchannel) working with chiller loop is used to condense the refrigerant. A shell and tube heat exchanger subcools the refrigerant. An external receiver is used to help controlling system pressure.

2.2 Coolant Loop

In most cases, water is the fluid used in the coolant loop. When a lower temperature is needed water in the coolant loop could be replaced by ethanol or glycol mixture. A pump with VFD controller is used to pump the fluid. A reservoir tank is installed at the suction of the pump in order to maintain a minimum suction pressure. The pressure at the discharge is measured by a pressure sensor and this signal is used to adjust the pump speed to maintain discharge pressure. Fluid is supplied to an inlet header from where it goes to each test/conditioning section. The fluid temperature at the inlet to test and conditioning sections is adjusted by a 530 W heater while the flow rate is adjusted by a stepper motor valve. The mass flow rate is measured by two CMF010 mass flow meters per test section and a DS006 mass flow meter for each conditioning section. Temperature measurements are done by T-type thermocouples inserted into the coolant tube. Coolant from test sections and conditioning sections returns to the outlet header. A plate heat exchanger and a 1.5 kW heater are installed after the header to adjust coolant temperature supplied to the pump.

2.3 Chiller Loop

The chiller loop provides cooling to the refrigerant sub-cooler, refrigerant condenser, and brazed plate heat exchanger in the coolant loop. The chiller loop consists of a chiller with pump and reservoir tank and now is running with 50%-50% ethylene-glycol water mixture. After the pump, glycol flows to a sub-cooler which subcools the refrigerant to make sure that liquid refrigerant flows into the gear pump. A 1.5 kW heater is used to adjust the condenser inlet temperature of glycol. A bypass has been made for the condenser to reduce pressure drop when the system is in evaporation mode. A plate heat exchanger is used for glycol so that the coolant loop can be cooled.

2.4 Data Reduction and Error Propagation

Table 1 Uncertainties of Measurements

εP	3.5 kPa
εDP	0.0015 to 0.04 kPa
εT	0.1 to 0.2 ºC
εm	0.1% to 0.15% of rate
$\varepsilon \rho$	0.0005 g-cm^{-3}

All instruments are calibrated with data loggers to reduce uncertainties. Thermocouples are calibrated in a stable NESLAB thermal bath with calibrated RTD thermometer as the reference. Pressure transducers are calibrated on the facility referenced by Fluke pressure calibrator 717. Mass flow meters are calibrated with 275 HART communicator by comparing set analogy signal and reading from the data loggers. The uncertainties are listed in Table 1 and details of facility and calibration process can be found in Li (2016). Heat transfer coefficient (HTC in W-m^{-2}K^{-1}) determined based on the wall temperature:

$$HTC = \frac{Q}{A_s(T_{wall} - T_{ref})} \tag{4}$$

In equation 4, *As* is the surface area which is the total port surface area in most cases. T_{wall} is a corrected wall temperature. T_{ref} is the bulk refrigerant temperature and is equal to saturation temperature in two-phase. *Q* is the total heat transfer rate which is measured in the coolant loop from knowing the flow rate and the temperatures at inlet and outlet of the block.

The pressure drop (PD in kPa m^{-1}) is determined by dividing differential pressure measurement and the length of the tube.

$$PD = \frac{DP}{L} \tag{5}$$

Based on NIST technical Note 1297, the overall uncertainty (εR) of a result (R) with a known function F of n variables x_i with known uncertainties (εx_i) could be expressed in equation 6a and 6b (Taylor and Kuyatt, 1994). This equation is under assumptions that all variables are independent, repeated measurements show Gaussian distribution, and all uncertainties of variables are in the same level of confidence. In this paper, the level of confidence is 95%.

$$R = F(x_1, x_2, \dots x_i, \dots)$$
$$\varepsilon R = \sqrt{\sum_{i=1}^{n} \left(\frac{\partial F}{\partial x_i}\varepsilon x_i\right)^2} \tag{6a, 6b}$$

3. MODELS USED FOR PREDICTION OF DATA

3.1 Pressure Drop in Refrigerant Two-phase Diabatic Flow-Homogeneous Approach

Carey (1992) introduced a simple homogenous model to model the frictional and momentum pressure drop. Hartnett and Kostic (1993) have developed a model to predict the fully developed laminar flow in rectangular ducts. The frictional pressure drop is represented as:

$$PD_{friction} = \frac{2fG^2}{D \times \rho_{TP}} \tag{7}$$

In equation 8, *f* is a non-dimensional number, the friction factor, determined implicitly from Hartnett and Kostic (1993). The accelerating pressure drop (PD_a) is the main contributor to momentum pressure drop which is defined as:

$$PD_a = \int \frac{dP}{dz} dz \tag{8}$$

$$\frac{dP}{dz} = \frac{d(\frac{x}{\rho_g} + \frac{1-x}{\rho_f})}{dz} \tag{9}$$

The accelerating pressure will be integrated along the heated length of the tube. Summary of 7 and 8 will be the predicted pressure drop.

3.2 Heat Transfer Coefficient in Flow Boiling – Predictions

Most correlations of two-phase evaporation heat transfer coefficient are developed for round tubes. Qu and Mudawar (2003) presented a correction to modify the round tube heat transfer coefficient prediction into a rectangular channel as equation 18.

$$HTC_{rec} = HTC_{round}\frac{Nu_3}{Nu_4} \tag{10}$$

Nu_3 and Nu_4 are the single-phase fully developed laminar Nusselt numbers for different wall heating conditions respectively.

$$Nu_3 = 8.235(1 - 1.883\beta + 3.767\beta^2 - 5.814\beta^3 + 5.361\beta^4 - 2.0\beta^5) \tag{11}$$

$$Nu_4 = 8.235(1 - 2.042\beta + 3.085\beta^2 - 2.477\beta^3 + 1.058\beta^4 - 0.186\beta^5) \tag{12}$$

Our data is compared to five models of HTC_{round} with correction to rectangular tube.

4. RESULTS AND DISCUSSIONS

4.1 Pressure Drop in Diabatic Evaporation Flow

The horizontal error bar in Figure 4 is the quality change in the test section. Each test run produces six pressure drop data points from test sections 1 to 6. In this run, the heat flux and mass flux in each test are identical for each test sections. When it is needed, constant wall temperature condition can be applied. When mass flux is fixed at 121 kg-m^{-2}s^{-1}, pressure drop slightly increases as the heat fluxes are increasing from1798 to 3608 Wm^{-2}. This is due to the fact that the accelerating pressure drop contributes more in the higher heat fluxes case. At the beginning, the pressure drop is small in the liquid phase in the bubbly flow. Pressure drop starts to increase as vapor quality goes higher. Figure 4 also shows the corresponding saturation pressure at each data points. The overall pressure drops from about 530 to 440 kPa from test section 1 to 6.

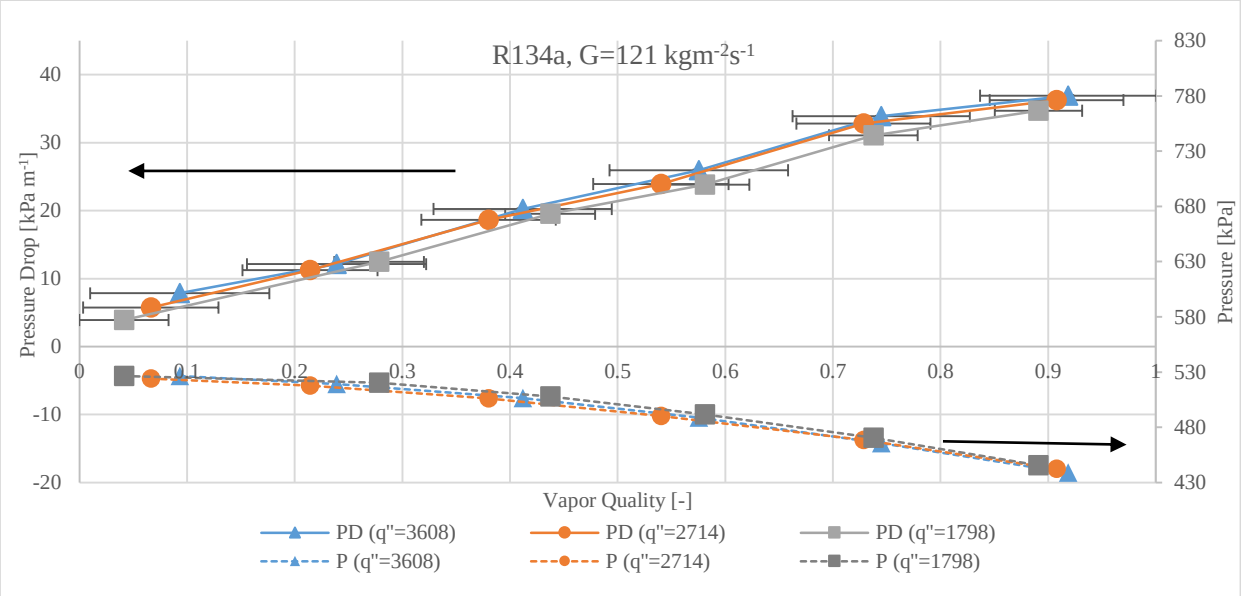

Figure 4 Diabatic pressure drop of R134a at fixed mass flux of 121 kg-m^{-2}s^{-1} and different heat fluxes under different vapor quality and saturation pressure

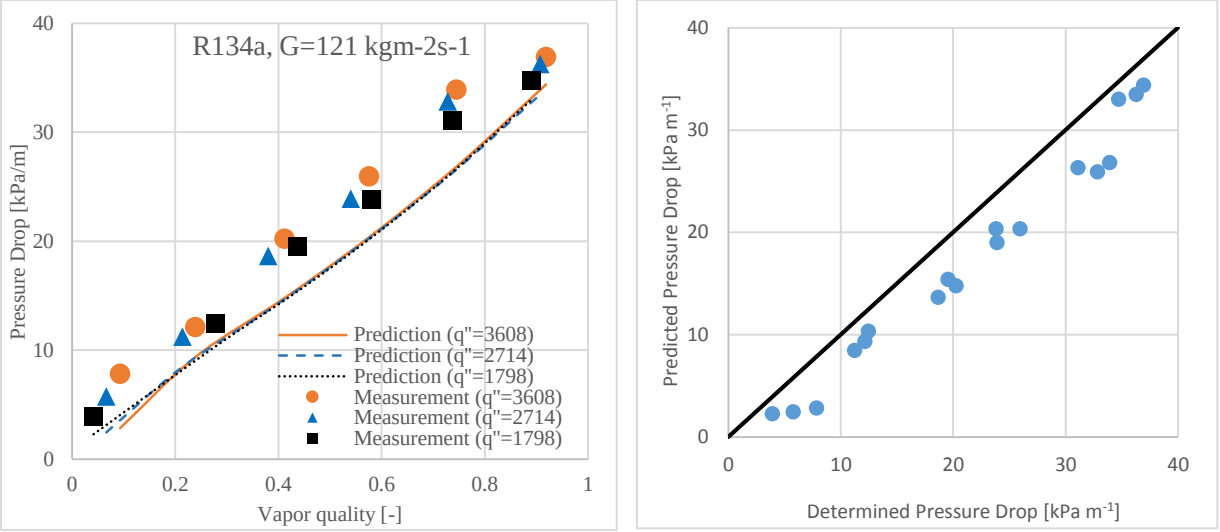

Figure 5 Pressure drop determined and comparison to the model

Figure 5 shows pressure drop measurements compared with the prediction of the homogeneous model (equation 7 and 8). The prediction shows lower values than the measurements. The mean absolute error (MAE) of the homogeneous model is 24% and the error is defined as:

$$MAE = \frac{\sum_{i=1}^{n} \left| \frac{Measurement - Prediction}{Measurement} \right|}{N} \times 100\% \quad (13)$$

4.2 Heat Transfer Coefficient

Figure 6 shows the heat transfer coefficient at fixed mass flux and for different heat fluxes as parameters. As with the pressure drop experiments, each line has six data points collected from test section 1 to 6. These heat transfer coefficient data points are gained at the same time of measuring pressure drop.

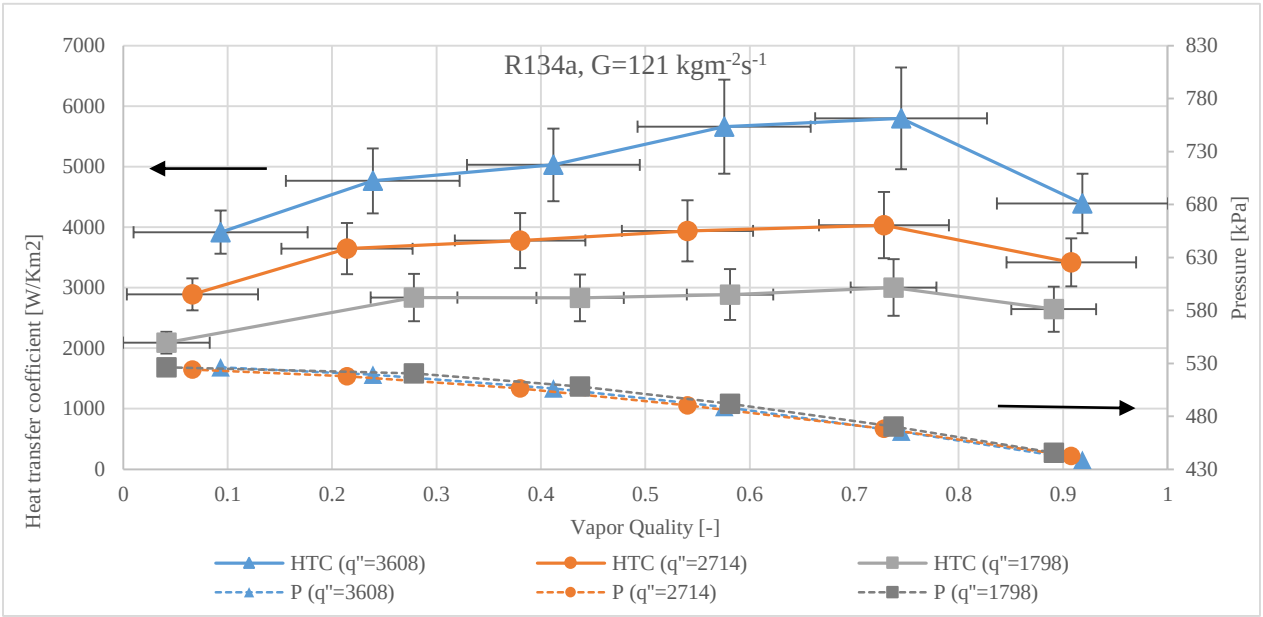

Figure 6 HTC at fixed mass flux of 121 kg-m^{-2}s^{-1} and different heat fluxes under different quality and saturation pressure

Three tests are conducted and each test has an identical mass flux of 121 $kgm^{-2}s^{-1}$. Heat transfer coefficient increases when the heat fluxes are increasing from 1798 to 3608 Wm^{-2}. As vapor quality increases, the heat transfer coefficient starts to increase. But the heat transfer coefficient is not a strong function of quality in a moderate range of quality (0.2 to 0.7) for low heat fluxes. At about the quality of 0.75, heat transfer coefficient reaches the highest value and starts to drop due to depression of boiling and dry out effects. HTC drops after it reaches the maximum points. The saturation pressure is also shown in figure 6. The pressure in test section 1 is about 530 kPa and in the last test section it is about 440 kPa. Data from the three tests are plotted with five heat transfer coefficient prediction model in Figure 7. It shows that all models have under-predicted the heat transfer coefficient. Figure 8 plots predicted heat transfer coefficient versus measurement.

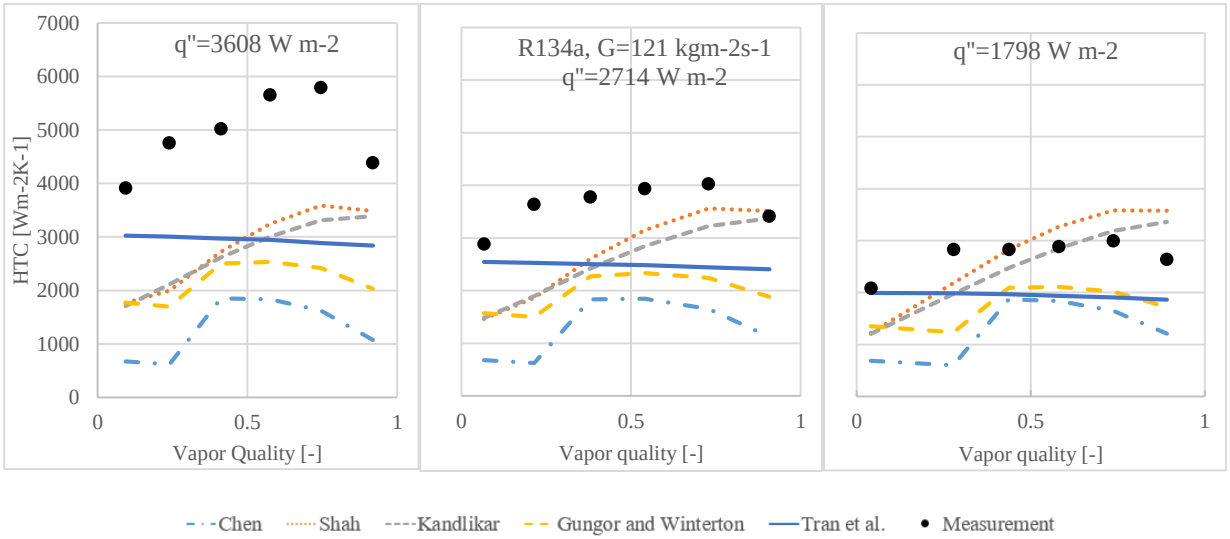

Figure 7 Comparison of measurement to prediction of the three tests

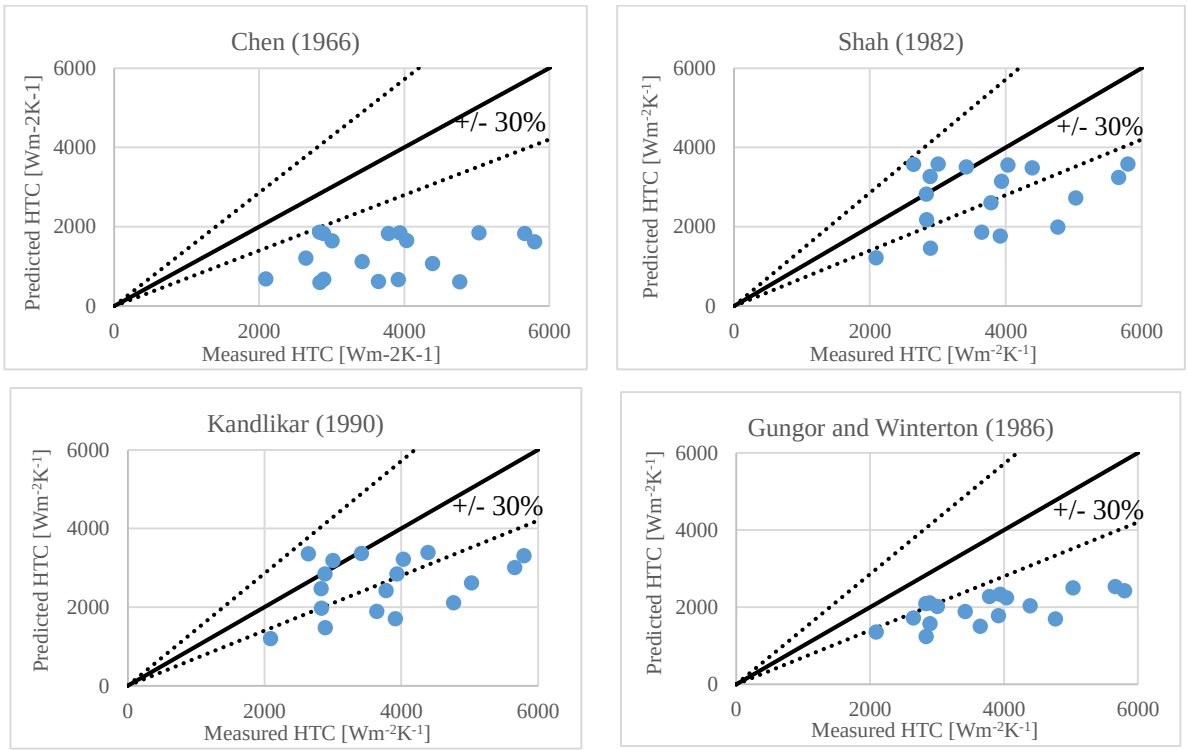

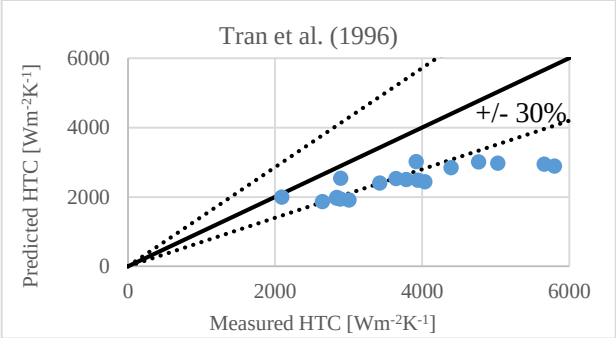

Figure 8 Comparison of prediction model to measurements

Figures 7 and 8, indicate that Chen (1966)'s model under predicts the heat transfer coefficient but with the same trends. The same situation for Gungor and Winterton (1986) can be observed. The models from Shah (1982) and Kandlikar (1990) predict an increasing curve till very high-quality zone. Tran et al. (1996) predict the enlargement of boiling effect at low quality but with a different trend over the whole quality change. Table 2 shows the 5 models and their MAE to measurement data.

Table 2 Each model and the mean absolute error

Model	MAE [%]
Chen (1966)	64.1
Shah (1982)	30.9
Kandlikar (1990)	31.9
Gungor and Winterton (1986)	45.2
Tran et al. (1996)	32.3

5. SUMMARY AND CONCLUSIONS

The paper presented a new type of experimental facility for microchannel heat transfer and pressure drop research in which R134a pressure drop and heat transfer coefficient are tested. The pressure drop increases with increasing of vapor quality. Higher heat flux increases slightly the pressure drop because of the increase in acceleration portion. The homogeneous model has an MAE of 24% in predicting pressure drop.

Five correlations used for comparison show reasonable but imperfect accuracy. Modified Shah (1982), Kandlikar (1990), and Tran et al. (1996) have about 30% of MAE when predicting heat transfer coefficient in this study. Gungor and Winterton (1986) has an MAE of 45%, and Chen (1966) is 64%.

The project is continuing and further analysis and data will follow.

NOMENCLATURE

A	area	m^2
β	aspect ratio	-
D	diameter	m
DP	differential pressure	kPa
f	friction factor	-
g	gravity	$m\ s^{-2}$
G	mass flux	$kg\ m^{-3}\ s^{-1}$
HTC	heat transfer coefficient	$W\ m^{-2}K^{-1}$
L	length	M
MAE	mean absolute error	%
Nu	Nusselt number	-
P	pressure	kPa

PD	pressure drop	kPa m^{-1}
Q	heat transfer rate	W
q''	heat flux	Wm^{-2}
ρ	density	kg m^{-3}
T	temperature	^oC
x	vapor quality	-

Subscript

a	acceleration
f	fluid
frictional	frictional
g	gas
rec	rectangular
ref	refrigerant
round	round
s	surface
TP	two phase
wall	wall

REFERENCES

Carey, V.P., (1992). Liquid-vapor phase-change phenomena, Hemisphere Publishing Co.

Chen, J. C. (1966). Correlation for boiling heat transfer to saturated fluids in convective flow. Industrial & Engineering Chemistry Process Design and Development, 5(3), 322–329.

Gungor, K.E. Winterton, R.H.S. (1986) A general correlation for flow boiling in tubes and annuli, Int. J. Heat Mass Transfer 29 351–358.

Harley, J. C. (1993). Compressible gas flows in microchannel and microjets. University of Pennsylvania.

Hartnett, J. P., & Kostic, M. (1989). Heat transfer to newtonian and non-newtonian fluids in rectangular ducts. Advances in Heat Transfer, 19, 247–356.

Kandlikar, S.G. (1990). A general correlation for saturated two- phase flow boiling heat transfer inside horizontal and vertical tubes, J. Heat Transfer 112 219–228.

Li, H. (2016). An Experimental Facility for Microchannel Research and Evaporating R134a in Microchannel Tube. University of Illinois.

Qu, W., & Mudawar, I. (2003). Flow boiling heat transfer in two-phase micro-channel heat sinks-I. Experimental investigation and assessment of correlation methods. International Journal of Heat and Mass Transfer.

Shah, M.M. (1982). Chart correlation for saturated boiling heat transfer: equations and further study, ASHRAE Trans. 88 185–196.

Taylor, B. N., & Kuyatt, C. E. (1994). Guidelines for Evaluating and Expressing the Uncertainty of NIST Measurement Results. Technology.

Tran, T.N. M.W. Wambsganss, D.M. France, (1996). Small circular- and rectangular-channel boiling with two refrig- erants, Int. J. Multiphase Flow 22 485–498.

Triplett, K. a., Ghiaasiaan, S. M., Abdel-Khalik, S. I., & Sadowski, D. L. (1999). Gas–liquid two-phase flow in microchannels Part I: two-phase flow patterns. International Journal of Multiphase Flow, 25(3), 377–394.

ACKNOWLEDGEMENT

This paper is a result of a project that was financially supported by the Air Conditioning and Refrigeration Center at the University of Illinois and its 30 member companies. CTS (Creative Thermal Solutions Inc.) provided the material, instrumentation and previous facility as a basis for the new, improved facility used to get presented data.